

Chapter 1

Pairing fluctuations and gauge symmetry restoration in rotating superfluid nuclei

Yoshifumi R. Shimizu

*Department of Physics, Faculty of Sciences, Kyushu University,
Fukuoka 812-8581, Japan*

Rapidly rotating nuclei provide us good testing grounds to study the pairing correlations; in fact, the transition from the superfluid to the normal phase is realized at high-spin states. The role played by the pairing correlations is quite different in these two phases: The static (BCS like mean-field) contribution is dominant in the superfluid phase, while the dynamic fluctuations beyond the mean-field approximation are important in the normal phase. The influence of the pairing fluctuations on the high-spin rotational spectra and moments of inertia is discussed.

1. Rotation and pairing correlations – Introduction

In all the different contributions in this Volume, various aspects of the pairing correlations, which play important roles in nuclear physics, are discussed. In this contribution I would like to concentrate on the effect of the pairing fluctuations in rapidly rotating nuclei,¹ which is generic and yet far from trivial. Here the pairing fluctuations mean the dynamic motions of the pairing gap, i.e., so-called the pairing vibrations² (see also Ref. 3), whose effects appear beyond the static (BCS) mean-field approximation and are characteristic in the finite system like atomic nucleus.

It is well known that most of non-closed shell nuclei, which have quadrupole deformed shape, exhibit collective nuclear rotations.⁴ In the 80's, the combined developments of the heavy-ion accelerators and the high-resolution γ -ray detectors made it possible to explore the properties of rapidly rotating nuclei, i.e., the high-spin states up to spin values $I \approx 60\hbar$, of medium and heavy nuclei. Many interesting phenomena and issues have been revealed; see e.g. Refs. 5–7, and Refs. 8,9 for more recent progress. The pairing correlations, either static or dynamic, play a crucial role in

most of these phenomena over the wide spin range. As for a well-known example, the superfluidity is responsible for the reduction of the moment of inertia for the collective nuclear rotation near the ground state;¹⁰ it takes only about (or even less than) half of the rigid-body value, which is expected for the independent nucleonic motions in the deformed mean-field. In this way, the ground states of deformed nuclei can be well described by the BCS theory with finite pairing gaps, $\Delta \approx 1$ MeV, and the BCS quasi-particles appear as a basic excitation mode. In fact, the “backbending” phenomenon,¹¹ which is systematically observed at spin $I \approx 10 - 16\hbar$ in the yrast^a bands of medium and heavy nuclei, can be understood as a band-crossing between the BCS vacuum and a specific two-neutron-quasiparticle excited configuration that is particularly favored by the effect of rotation¹² (see the contribution of F. Stephens and I.-Y. Lee and that of P. Ring to this volume). After the understanding of this novel phenomenon, it was realized that not only the yrast band but also many excited rotational bands can be well described by the concept of independent quasiparticle excitations in the rotating frame.¹³ This is quite nontrivial; complex rotational spectra at high-spin states can be nicely described by the so-called cranked shell model¹⁴ (see the contribution of S. Frauendorf to this Volume), which is one of the most important achievements in the studies of rapidly rotating nuclei.

The Cooper pair in nucleus is composed of a pair of nucleons in the time-reversal conjugate orbits whose angular momenta couple to $J = 0$.^b The effect of rotation, which appears as the Coriolis and centrifugal forces in the rotating frame, tends to align the angular momenta of nucleonic orbits to the rotation axis, and consequently breaks the Cooper pairs. In analogy to the metallic superconductors in the magnetic field, it was predicted that the phase transition from the superfluid to the normal phase is induced by the rapid rotation.¹⁵ However, a sharp transition as in macroscopic systems would not be expected in a finite system such as the nucleus. Instead, the finite nuclear system provides the opportunities to study a “phase transition” in terms of the individual quantum states such as the rotational-band spectra with non-negligible effects of the dynamic fluctuations. In fact, the transition is not very simple even within the mean-field approximation: The effect of the band-crossings (backbendings), i.e., the successive excita-

^a The word “yrast” means dizziest, and the yrast state is the lowest energy state at a given angular momentum. Connecting the yrast states composes the yrast band.

^b The nucleon pairs with higher multipole, e.g. the quadrupole pair ($J = 2$), also play important roles especially in deformed nuclei.

tions (alignments) of quasiparticles, is more dramatic,¹⁶ and the calculated pairing gap reduces stepwisely along the yrast states. It is now believed that the unpaired phase is realized for neutrons at spins $I \approx 20 - 30\hbar$ in the rare-earth region, evidence for which is given by comparing the observed spectra with the rotating single-particle energies with zero pairing gap.^{17,18} However, it was recognized that the effects of pairing correlations remain considerably after vanishing the static (BCS) pairing gap;^{19,20} the “effective pairing gap” including the dynamic fluctuations beyond the static mean-field does not vanish and only gradually decrease across the phase transition.^{1,19}

In the following, after briefly reviewing how to treat the nuclear rotational motion, I discuss the theoretical method to evaluate the pairing fluctuations within the random phase approximation (RPA).^{21,22} A few examples of the calculated results, taken from our studies in Refs. 1,23–27, are presented in comparison with experimental data.

2. Description of rotational motion – Cranking model

In order to make this article self-contained, here I recapitulate the method to treat the rotational motion and to analyse the rotational spectra; see e.g. Refs. 5,6,13,14 for detailed accounts.

The nuclear collective motion is treated semiclassically, which is called the “cranking” prescription.²⁸ Namely the Hamiltonian of the system is transformed into the *uniformly* rotating frame^c,

$$\hat{H}' = \hat{H} - \omega_{\text{rot}} \hat{J}_x, \quad (1)$$

where ω_{rot} denotes the rotational frequency about the rotation axis (x -axis), which is chosen to be one of the principal axes of the deformed body with largest moment of inertia, and is usually perpendicular to the symmetry axis of the quadrupole nuclear shape. Since we are mainly interested in the lowest energy (yrast) high-spin states, this is a natural assumption (see Ref. 8 for more general situations). The energy in the rotating frame $E' = \langle H' \rangle$, which is called the “routhian”, and the angular momentum along the rotation axis, $I_x = \langle \hat{J}_x \rangle = -\partial E' / \partial \omega_{\text{rot}}$ with $I_x = \sqrt{I(I+1)} \approx I + \frac{1}{2}$, are evaluated as functions of the rotational frequency ω_{rot} .

On the other hand, the nuclear collective rotation is measured as the rotational spectra, $E(I)$, which are composed of a group of states with different angular momentum I changing by two units ($\Delta I = 2$), and connected

^c $\hbar = 1$ unit is used for mathematical expressions.

by the strong electric quadrupole ($E2$) γ -ray emissions. In accordance with the simple assumption of rotational motion in Eq. (1), the rotational frequency is calculated by

$$\omega_{\text{rot}}(I) = \frac{\partial E}{\partial I} \approx \frac{E(I+1) - E(I-1)}{(I+1) - (I-1)} = \frac{1}{2}E_\gamma, \quad (2)$$

with the γ -ray energy E_γ of the associated rotational transition. This implicitly defines the relation $I_x(\omega_{\text{rot}})$, between the angular momentum I_x and the rotational frequency ω_{rot} , and then the experimental routhian $E'(\omega_{\text{rot}})$ is obtained as

$$E'(\omega_{\text{rot}}) = E(I(\omega_{\text{rot}})) - \omega_{\text{rot}}I_x(\omega_{\text{rot}}). \quad (3)$$

In this way the theoretical routhians can be directly compared with the experimental routhians, although the latter are given only at the discrete points of the rotational frequencies.

In the mean-field approximation, e.g., in the cranked shell model, the Hamiltonian \hat{H} is replaced with the one-body Hamiltonian,

$$\hat{H} \rightarrow \hat{h} = \hat{h}_{\text{def}} - \Delta(\hat{P}^\dagger + \hat{P}) - \lambda\hat{N}, \quad (4)$$

where \hat{h}_{def} describes the single-particle motion in the deformed average potential, the second term is the pair-field with \hat{P}^\dagger being the monopole pair creation operator,

$$\hat{P}^\dagger = \frac{1}{2} \sum_i \hat{c}_i^\dagger \hat{c}_{\tilde{i}}^\dagger \quad (\tilde{i}: \text{time reversed orbit of } i), \quad (5)$$

and the last term $-\lambda\hat{N}$ ensures the correct particle number on average, because the number conservation is broken in the BCS treatment. By diagonalizing the cranking Hamiltonian with Eq. (4) the quasiparticle energies in the rotating frame are obtained, which can be directly compared with the complex rotational spectra for both even and odd nuclei;¹⁴ see the contribution of S. Frauendorf to this volume for detailed explanations. Of course, it can be well used with $\Delta = 0$ for the case of quenched pairing correlations, i.e., for the normal phase routhians.

3. Pairing fluctuations with RPA method

The dynamic pairing fluctuations beyond the mean-field approximation is induced by the two-body interaction. The simple one, the so-called monopole pairing force, is employed with the operator \hat{P}^\dagger defined in Eq. (5);

$$\hat{H} = \hat{h}_{\text{def}} + \hat{V}, \quad \hat{V} = -\frac{G}{2}(\hat{P}^\dagger \hat{P} + \hat{P} \hat{P}^\dagger), \quad (6)$$

with the strength G . The BCS treatment of this Hamiltonian leads to the one-body Hamiltonian in Eq. (4) with the *selfconsistent* (static) pairing gap $\Delta = G\langle\hat{P}^\dagger\rangle_{\text{mf}} = G\langle\hat{P}\rangle_{\text{mf}}$, which is nothing else but the order parameter of the super-to-normal phase transition.

The fluctuations about the mean-field are calculated by diagonalizing the Hamiltonian (6) within the RPA. The induced energy gain is given by

$$E_{\text{corr}}^{\text{RPA}} = \frac{1}{2} \left[\sum_n \omega_n - \sum_{\alpha>\beta} (e_\alpha + e_\beta) \right], \quad (7)$$

where ω_n is the RPA eigenenergy and e_α is the quasiparticle (particle or hole) energy in the superfluid (normal) phase. They are calculated with the cranking prescription (1) as functions of ω_{rot} to study the rapidly rotating nuclei. Thus, the total RPA routhian is calculated as

$$E'_{\text{RPA}} = E'_{\text{mf}} + E_{\text{corr}}^{\text{RPA}}, \quad E'_{\text{mf}} = \langle \hat{h}_{\text{def}} - \omega_{\text{rot}} \hat{J}_x \rangle_{\text{mf}} - G\langle \hat{P}^\dagger \rangle_{\text{mf}}^2. \quad (8)$$

It should be mentioned that $E_{\text{corr}}^{\text{RPA}}$ in Eq. (7) contains the exchange energy, $E_{\text{ex}} = \langle \hat{V} \rangle_{\text{mf}} + G\langle \hat{P}^\dagger \rangle_{\text{mf}}^2$, which is found to be rather constant¹ against the change of ω_{rot} . Note that the calculation of $E_{\text{corr}}^{\text{RPA}}$ requires all the RPA eigenenergies, which amount to a few or more than ten thousands depending on the pairing model space. Since the convergence with respect to the number of solutions is slow,²⁹ it is important to include all of them for stable results, which is a numerically demanding task. A general efficient method to perform the calculation was developed in Ref. 1 by utilizing the linear response theory, and it was further improved in Ref. 27.

3.1. Response function technique

Generally the two-body interaction can be represented by the form of multi-component separable force,

$$\hat{V} = -\frac{1}{2} \sum_{\rho=1}^q \chi_\rho \hat{Q}_\rho \hat{Q}_\rho, \quad Q_\rho^\dagger = Q_\rho, \quad (9)$$

with Hermitian one-body operators \hat{Q}_ρ and strengths χ_ρ ($\rho = 1, 2, \dots, q$). For the monopole pairing interaction (6), $q = 2$ and $\hat{Q}_1 \equiv \hat{P}^\dagger + \hat{P}$, $i\hat{Q}_2 \equiv \hat{P}^\dagger - \hat{P}$, and $\chi_1 = \chi_2 \equiv G/2$. The RPA eigenvalue problem can then be replaced to solve the following dispersion equation,

$$\det \mathcal{R}(\omega) = 0, \quad \text{with} \quad \mathcal{R}(\omega) = [1 - R(\omega)\chi]^{-1}R(\omega), \quad (10)$$

where the $q \times q$ matrices, $\mathcal{R}(\omega)$ and $R(\omega)$, are composed of the RPA and the unperturbed response functions for the operators \hat{Q}_ρ , and the diagonal matrix $\chi = (\delta_{\rho\sigma}\chi_\rho)$;

$$R_{\rho\sigma}(\omega) \equiv \sum_{\alpha>\beta} \left[\frac{q_\rho^*(\alpha\beta)q_\sigma(\alpha\beta)}{e_\alpha + e_\beta - \omega} + \frac{q_\rho(\alpha\beta)q_\sigma^*(\alpha\beta)}{e_\alpha + e_\beta + \omega} \right], \quad (11)$$

with $q_\rho(\alpha\beta) \equiv \langle \alpha\beta | \hat{Q}_\rho | 0 \rangle_{\text{mf}}$. Then, by employing the adiabatic turn-on the interaction and the analytic property of the response function (11), it was shown that the correlation energy can be calculated by the following formula,²⁷

$$E_{\text{corr}}^{\text{RPA}} = \frac{1}{2\pi} \int_0^\infty \text{Re}[\log\{\det[1 - R(i\omega)\chi]\}] d\omega, \quad (12)$$

so that it is *not* necessary to explicitly solve Eq. (10). Note that the integration is taken along the upper imaginary axis $z = i\omega$ in the complex energy plane, for which the integrand is a smoothly decreasing function and the numerical integration can be done straightforwardly. In Ref. 1 a different integration path is taken near the positive real axis, where the integrand is a oscillating function, and the numerical integration should have been done more carefully (see Ref. 1,27 for detailed discussions).

It is instructive to consider the following RPA pairing gap,^{1,25,27}

$$\Delta_{\text{RPA}} = G \sqrt{\frac{1}{2} \sum_n \left[\langle 0 | \hat{P}^\dagger | n \rangle \langle n | \hat{P} | 0 \rangle + \langle 0 | \hat{P} | n \rangle \langle n | \hat{P}^\dagger | 0 \rangle \right]_{\text{RPA}}}, \quad (13)$$

in keeping with Δ_{NP} introduced in the variation after number projection (NP) approach¹⁹ (see §3.4). However, the contribution of the zero mode, i.e., the symmetry recovering Nambu-Goldstone (NG) mode (the pairing rotation³), which is present in the superfluid phase, diverges because of the small amplitude approximation inherent in the RPA: It is natural to replace its (divergent) contribution to that of the mean-field;

$$\frac{1}{2} \left[|\langle 0 | \hat{P}^\dagger | n \rangle|^2 + |\langle 0 | \hat{P} | n \rangle|^2 \right]_{n=\text{NG}} \rightarrow \langle \hat{P}^\dagger \rangle_{\text{mf}} \langle \hat{P} \rangle_{\text{mf}} = (\Delta/G)^2. \quad (14)$$

Then the difference between the squared RPA and mean-field pairing gaps, $\Delta_{\text{RPA}}^2 - \Delta^2$, represents the effect of pairing vibrations, which can be calculated by integrating the trace of the RPA response matrix $\text{Tr}\mathcal{R}(\omega)$ without explicitly solving the RPA equation.^{1,25,27}

In Fig. 1, an example of the RPA correlation energy and the pairing gaps are shown. The mean-field pairing gap Δ reduces stepwisely to zero at the critical frequency $\omega_{\text{rot}} = \omega_c \approx 0.33$ MeV of the super-to-normal

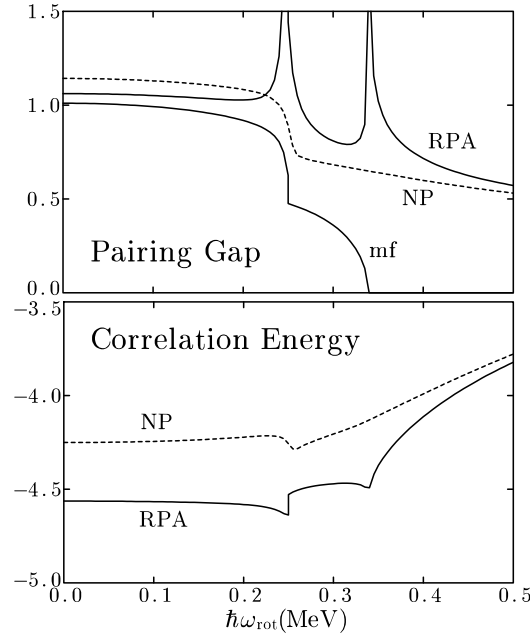


Fig. 1. The RPA and BCS mean-field (mf) pairing gaps (upper) and the RPA correlation energies (lower) for neutrons in the yrast band of ^{164}Er as functions of the rotational frequency ω_{rot} . The results by the variation after number projection (NP) method are included as dashed lines. Here the exchange contributions are excluded^{19,25} both in Δ_{RPA} and Δ_{NP} . Taken from Ref. 27 with eliminating two irrelevant lines.

phase transition. The first reduction at $\omega_{\text{rot}} \approx 0.24$ MeV is caused by the two-neutron-quasiparticle alignments (excitations) related to the back-bending phenomenon, where the correlation energy $E_{\text{corr}}^{\text{RPA}}$ is discontinuous. At $\omega_{\text{rot}} = \omega_c$ it is continuous but its derivative, i.e., the correction to the alignment, $\delta I_x = -\partial E_{\text{corr}}^{\text{RPA}} / \partial \omega_{\text{rot}}$, diverges, which is a drawback of the RPA and one has to go beyond the RPA²³ or to make smooth interpolations to compare with the experimental data. At these two frequencies the RPA gap Δ_{RPA} diverges, because one of the RPA eigenenergies goes across zero. It should be mentioned that $E_{\text{corr}}^{\text{RPA}}$ is almost constant as long as the BCS pairing gap is sizable, while its absolute value decreases after its quenching; therefore the effect of $E_{\text{corr}}^{\text{RPA}}$ is important after the static pairing gap becomes small. In contrast to the mean-field gap, Δ_{RPA} keeps finite values even at highest frequencies, reflecting that the pairing fluctuations remains considerably in the normal phase. These behaviors of the correlation energy and the pairing gaps are rather general in rapidly rotating nuclei.¹

3.2. Routhians and alignments in normal deformed nuclei

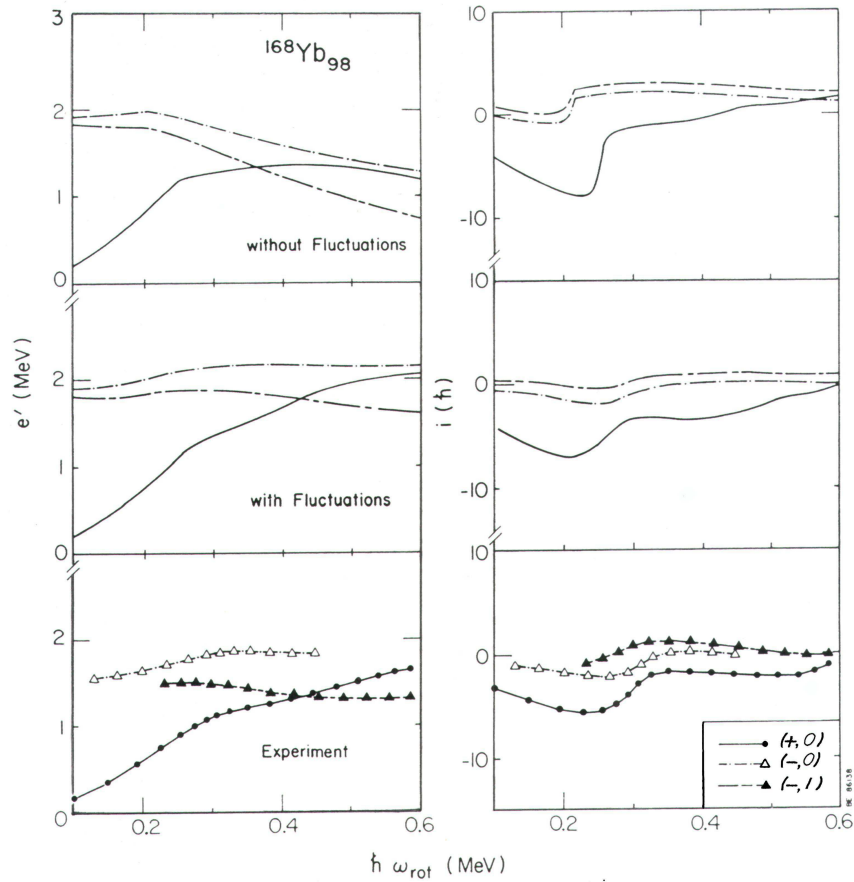


Fig. 2. Calculated and experimental routhians e' (left-hand side) and alignments i (right-hand side) for the lowest three configurations in ^{168}Yb ; the top panels display the calculation without fluctuations, middle with fluctuations, and bottom experimental data. Taken from Ref. 1.

In order to discuss how the correlation energy affects rotational spectra at high-spin states, the routhians e' and the aligned angular momenta (“alignments”) i for the lowest three configurations in the nucleus ^{168}Yb are shown in comparison with experimental data in Fig. 2. Here these quantities are plotted relative to the so-called rigid-body reference, i.e.,

$$e'(\omega_{\text{rot}}) = E'(\omega_{\text{rot}}) + \frac{1}{2} \mathcal{J}_0 \omega_{\text{rot}}^2, \quad i(\omega_{\text{rot}}) = I_x(\omega_{\text{rot}}) - \mathcal{J}_0 \omega_{\text{rot}}, \quad (15)$$

where \mathcal{J}_0 is the rigid-body moment of inertia. In this calculation with a rather simple interaction in Eq. (6) the experimental moment of inertia cannot be described correctly, and the \mathcal{J}_0 value for theoretical results is adjusted so as to reproduce the lower frequency part of routhians e' , for which the correlation energy remains almost constant as it is shown in Fig. 1. Apparently, the calculated routhians of the higher frequency part is smaller than the experimental data without the pairing fluctuations. The $(+, 0)$ configuration is the band with positive parity and even spins and corresponds to the yrast band; the kink of its routhian at $\omega_{\text{rot}} \approx 0.28$ MeV corresponds to the two-neutron-quasiparticle crossing. In this band the mean-field pairing gap almost quenches around $\omega_{\text{rot}} \approx 0.4$ MeV, and certainly the effect of the pairing fluctuations becomes more evident at larger frequencies. The negative parity excited bands with $(-, 0)$ and $(-, 1)$ are two neutron excited configurations and their pairing gaps are about 60% of the $(+, 0)$ band at lowest frequency. Therefore, their static pairing correlations are reduced more than that of the $(+, 0)$ band, and the effects of pairing fluctuations are more conspicuous in the relatively lower frequency region. With these effects of the fluctuations, the overall agreement between the calculation and the experiment apparently improves. From the general dependence of $E_{\text{corr}}^{\text{RPA}}$ on ω_{rot} , the correction to the alignments i is always negative, which is called “dealignment”, and it amounts to $2 - 3\hbar$; again, this makes the agreement of alignments much better.

3.3. Moments of inertia in superdeformed nuclei

It was also discussed²⁴ that the pairing fluctuations play important roles in the nuclei with very large deformation, which are called “superdeformation” and very regular rotational bands have been systematically observed; see Refs. 30,31 and the contribution of P.-H. Heenen to this Volume.

For the analysis of these superdeformed bands, the two moments of inertia are utilized quite often; they are called the kinematic and dynamic inertia, $\mathcal{J}^{(1)}$ and $\mathcal{J}^{(2)}$, respectively, and are defined by

$$\mathcal{J}^{(1)} \equiv \frac{I_x}{\omega_{\text{rot}}} = -\frac{1}{\omega_{\text{rot}}} \frac{\partial E'}{\partial \omega_{\text{rot}}}, \quad \mathcal{J}^{(2)} \equiv \frac{\partial I_x}{\partial \omega_{\text{rot}}} = -\frac{\partial^2 E'}{\partial^2 \omega_{\text{rot}}}. \quad (16)$$

The corrections induced by the pairing fluctuations to these inertia, $\delta\mathcal{J}^{(1)} = -(1/\omega_{\text{rot}})(\partial E_{\text{corr}}/\partial \omega_{\text{rot}})$ and $\delta\mathcal{J}^{(2)} = -\partial^2 E_{\text{corr}}/\partial^2 \omega_{\text{rot}}$, are schematically depicted in Fig. 3. Here the symbol ω^* denotes the frequency of the inflection point in the correlation energy and is located, in most cases, near the critical frequency of the pairing phase transition.

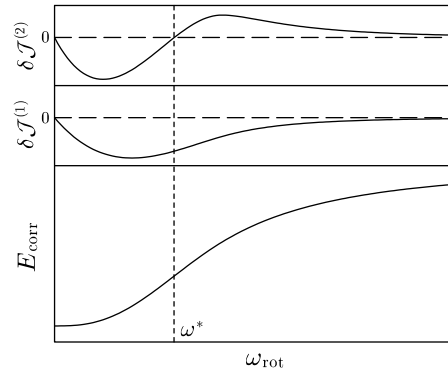


Fig. 3. Schematic figure depicting the (smoothed) pairing correlation energy and its influence on the two moments of inertia $\mathcal{J}^{(1)}$ and $\mathcal{J}^{(2)}$.

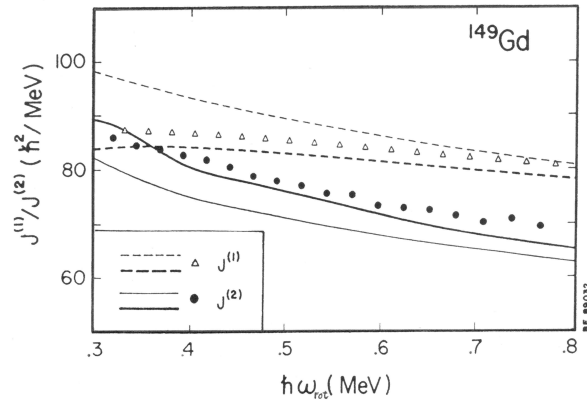


Fig. 4. Calculated and experimental moments of inertia $\mathcal{J}^{(1)}$ and $\mathcal{J}^{(2)}$ for the yrast superdeformed band in ^{149}Gd ; thick (thin) lines denote the result with (without) pairing fluctuations by using the RPA method. Taken from Ref. 24.

The superdeformed nuclei are realized by the strong shell effects based on the special deformations, e.g., the integer axis ratio like 2 : 1, and reflect the characteristics of the deformed closed shell. Therefore, just as in the case of the magic nuclei, the pairing correlations are very much reduced. Especially, those in the mass number $A \approx 150$ region are believed to be in the normal phase ($\Delta = 0$) already in their lowest states, and then the inflection point ω^* in Fig. 3 is expected to be lower than the experimentally observed frequency region. Thus, the corrections to the inertia is negative for $\mathcal{J}^{(1)}$ and positive for $\mathcal{J}^{(2)}$. In Fig. 4, the calculated and experimental inertia are compared for the yrast superdeformed band of ^{149}Gd . The mean-field

calculation overestimates $\mathcal{J}^{(1)}$ while it underestimates $\mathcal{J}^{(2)}$, and a good agreement is obtained by including the effects of pairing fluctuations; again this is rather generic for superdeformed nuclei in the $A \approx 150$ region.²⁴

3.4. Gauge symmetry restoration

In the RPA the broken symmetry is signalled by the appearance of the zero-energy NG mode, whose contribution to the correlation energy is largest, $\approx 2\Delta$, from Eq. (7). This implies the importance of restoring the gauge symmetry (the number conservation); the method is called the number projection, which explicitly projects out wave functions with good particle numbers from a gauge-symmetry broken wave function. In fact, it has been known²² that the correlations beyond the mean-field approximation can be taken into account by optimizing the superfluid mean-field wave function from which the projection is carried out; the so-called variation after projection (VAP) approach. Therefore the variation after number projection (NP) is an alternative method to evaluate the pairing fluctuations in the rotating nuclei (see the contribution of J. L. Egido to this Volume).

Since the expectation value of the monopole pairing operator \hat{P}^\dagger vanishes for the number conserving wave function, the NP pairing gap is defined by the following;¹⁹

$$\Delta_{\text{NP}} = G\sqrt{\frac{1}{2}(\langle \hat{P}^\dagger \hat{P} \rangle_{\text{NP}} + \langle \hat{P} \hat{P}^\dagger \rangle_{\text{NP}})}. \quad (17)$$

The correlation energy and the pairing gap evaluated by the NP approach are also included in Fig. 1. It can be seen that both quantities behave quite similarly to those evaluated by the RPA method, although the NP correlation energy is smaller indicating that the RPA method takes more correlations into account. In Ref. 25 comparison of the RPA and NP methods were performed for the routhians and alignments in rapidly rotating nuclei, and it was found that indeed two methods give very similar results. A merit of the NP method is that its result is smooth across the critical point of the super-to-normal phase transition in contrast to the RPA. It is especially useful to calculate the $\mathcal{J}^{(1)}$ and $\mathcal{J}^{(2)}$ inertias, which require the first and second derivatives of the correlation energy. An example is shown in Fig. 5, where the NP method is applied²⁶ to the yrast superdeformed band in ^{190}Hg . The $\mathcal{J}^{(2)}$ inertias of the superdeformed nuclei in the mass number $A \approx 190$ region systematically show increasing behaviors as ω_{rot} . Because of smaller shell gaps than those in the $A \approx 150$ regions, the stronger pairing correlations are expected. Namely the inflection point ω^*

in Fig. 3 is in the higher frequency range that is experimentally observed, and then the increasing trends of $\mathcal{J}^{(1)}$ and $\mathcal{J}^{(2)}$ can be obtained by the NP approach without recourse to the smooth interpolation, which is necessary for the RPA.

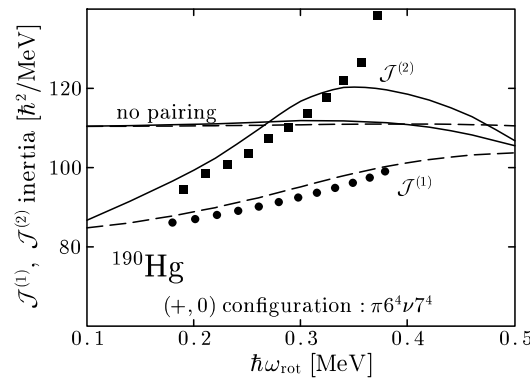


Fig. 5. Calculated and experimental moments of inertia $\mathcal{J}^{(1)}$ and $\mathcal{J}^{(2)}$ for the yrast superdeformed band in ^{190}Hg by using the variation after number projection method. Taken from Ref. 26 but with newer experimental data.

4. Summary

In this contribution I explained how the effects of the pairing fluctuations appear in rapidly rotating nuclei. By making use of the response function technique, the correlation energy induced by the pairing fluctuations can be evaluated within the RPA method. The calculated RPA correlation energy is rather constant as long as the static pairing gap is sizable, but its absolute value decreases after the static gap is quenched. In this way, the pairing fluctuations result in dealignments of about a few units with respect to the mean field calculation, which makes the agreements with experimental data much better in both normal deformed and superdeformed nuclei. Thus, the effects of the pairing fluctuations are important especially after the normal phase being realized at high-spin states.

Acknowledgements

I express sincere gratitude to collaborators in the related works. Especially, I am deeply in debt to Jerry D. Garrett for inspiring discussions and understanding experimental data, who passed away in August, 1999.

References

1. Y. R. Shimizu, J. D. Garrett, R. A. Broglia, M. Gallardo, and E. Vigezzi, *Rev. Mod. Phys.* **61**, 131 (1989).
2. D. Bes and R. A. Broglia, *Nucl. Phys. A* **80**, 289 (1966).
3. R. A. Broglia, O. Hansen, and C. Riedel, *Adv. Nucl. Phys.* **6**, 287 (1973).
4. A. Bohr and B. R. Mottelson, *Nuclear Structure*, Vol.II (Benjamin, New York, 1975).
5. H. J. A. Voigt, J. Dudek, and Z. Szymanski, *Rev. Mod. Phys.* **55**, 949 (1983).
6. Z. Szymanski, *Fast Nuclear Rotation* (Oxford University Press, 1984).
7. J. D. Garrett, G. B. Hagemann, and B. Herskind, *Ann. Rev. Nucl. Part. Sci.* **36**, 419 (1986).
8. S. Frauendorf, *Rev. Mod. Phys.* **73**, 463 (2001).
9. W. Satula and R. A. Wyss, *Rep. Prog. Phys.* **68**, 131 (2005).
10. A. Bohr, B. R. Mottelson, and D. Pines, *Phys. Rev.* **110**, 936 (1958).
11. A. Johnson, H. Ryde, and J. Sztarkier, *Phys. Lett. B* **34**, 605 (1971).
12. F. S. Stephens and R. S. Simon, *Nucl. Phys. A* **183**, 257 (1972).
13. R. Bengtsson and S. Frauendorf, *Nucl. Phys.* **A327**, 139 (1979).
14. R. Bengtsson, S. Frauendorf, and F.-R. May, *At. Data Nucl. Data Table* **35**, 15 (1986).
15. B. R. Mottelson and J. G. Valatin, *Phys. Rev. Lett.* **5**, 511 (1960).
16. Y. R. Shimizu and K. Matsuyanagi, *Prog. Theor. Phys.* **70**, 319 (1983).
17. J. D. Garrett, in *Nuclear Structure 1985*, edited by R. A. Broglia, G. B. Hagemann, and B. Herskind (North-Holland, Amsterdam, 1985), p.111.
18. J. C. Bacelar, M. Diebel, C. Ellegaard, J. D. Garrett, G. B. Hagemann, B. Herskind, A. Holm, C.-X. Yang, and J.-Y. Zhang, *Nucl. Phys.* **A442** (1985), 509.
19. J. L. Egido, P. Ring, S. Iwasaki, and H. J. Mang, *Phys. Lett. B* **154**, 1 (1985).
20. R. A. Broglia, M. Diebel, S. Frauendorf, and M. Gallardo, *Phys. Lett. B* **166**, 252 (1986).
21. A. L. Fetter and J. D. Walecka, *Quantum Theory of Nuclear Many-Particle Systems* (McGraw-Hill, New York, 1971).
22. P. Ring and P. Schuck, *The Nuclear Many-Body Problem* (Springer-Verlag, Berlin, 1980).
23. Y. R. Shimizu and R. A. Broglia, *Nucl. Phys.* **A476**, 228 (1988).
24. Y. R. Shimizu, E. Vigezzi, and R. A. Broglia, *Nucl. Phys.* **A509**, 80 (1990).
25. Y. R. Shimizu and R. A. Broglia, *Nucl. Phys.* **A515**, 38 (1990).
26. Y. R. Shimizu, *Nucl. Phys.* **A520**, 477c (1990).
27. Y. R. Shimizu, P. Donati, and R. A. Broglia, *Phys. Rev. Lett.* **85**, 2260 (2000).
28. D. R. Inglis, *Phys. Rev.* **96**, 1059 (1954); **103**, 1786 (1956).
29. J. L. Egido, H. J. Mang, and P. Ring, *Nucl. Phys.* **A341**, 229 (1980).
30. P. J. Nolan and P. J. Twin, *Ann. Rev. Nucl. Part. Sci.* **38**, 533 (1988).
31. R. V. F. Janssens and T. L. Khoo, *Ann. Rev. Nucl. Part. Sci.* **41**, 321 (1991).